



# Oxovanadium complexes catalyzed oxidation of lignin and lignin dimers in acetonitrile/water under O<sub>2</sub>

Chao Liu<sup>1</sup> · Fei Lin<sup>1</sup> · Xiangchen Kong<sup>1</sup> · Yuyang Fan<sup>1</sup> · Weicong Xu<sup>1</sup> · Rui Xiao<sup>1</sup>

Received: 16 October 2021 / Revised: 25 November 2021 / Accepted: 30 November 2021 / Published online: 15 January 2022  
© The Author(s), under exclusive licence to Springer-Verlag GmbH Germany, part of Springer Nature 2021

## Abstract

Selective oxidation of lignin is increasingly investigated due to its advantage of retaining the aromatic rings to produce value-added platform chemicals. In this paper, oxovanadium complexes catalyzed oxidation of lignin and lignin dimers in acetonitrile/water system under O<sub>2</sub> was reported. Under optimal conditions of VO(acac)<sub>2</sub> catalyzed oxidation, 95 mol% of lignin dimer 2-phenoxy acetophenone was converted, producing 43 mol% of phenol and 83 mol% of benzoic acid. The catalytic ability of V(acac)<sub>3</sub> was higher than that of VO(acac)<sub>2</sub>, but it caused heavier repolymerization and lower product yields. VO(acac)<sub>2</sub> catalyzed oxidation system also cleaved various β-O-4 lignin dimers, achieving >95 mol% conversion. Whereas, yields of phenols from these dimers were lower than 5 mol%. These phenolics were shown to polymerize under reaction conditions. Furthermore, this oxidation system depolymerized poplar organosolv lignin. After oxidation, aromatic and C-O aliphatic functionalities in the heavy fractionation largely disappeared, and the weight-average molecular weight decreased from 5720 to 1140 Da.

**Keywords** Lignin · Oxidation · Oxovanadium complexes · Homogeneous catalysis

## 1 Introduction

Lignin is the only abundant and renewable aromatic resource in nature. It is an alternative source to fossil resources for value-added aromatic chemicals [1], mainly methoxylated phenolic platform compounds [2–4]. As one of the three main components of lignocellulosic biomass (cellulose, lignin, and hemicellulose), lignin accounts for 15–35% of the mass and 40% of the energy [2, 5]. Lignin is a polymer of *p*-hydroxyphenyl, guaiacyl, and syringyl units linked

through various C–C and C–O bonds, and its structure varies by the biomass feedstocks and isolation methods [4, 6, 7]. Meanwhile, the annual production of technical lignin, mainly from pulping and lignocellulosic bioethanol industries, is over 50 million tons [8].

Lignin is an underutilized carbon source. Its usage is limited and only 5% of lignin is used for other purposes besides heat and power [1, 2, 8]. With the continuous development of biorefinery technologies, conversion and utilization of lignin has gradually attracted people's attention [2–4, 6, 9–13]. Pyrolysis, hydrogenation, and oxidation are three common methods for lignin conversion. Pyrolysis can rapidly degrade lignin into small molecular fragments, but the coupling condensation, as well as coke and char formation, is prominent, which leads to the low yields and low selectivity of aromatic products [14–16]. Hydrogenation can efficiently cleave C–O and/or C–C bonds within lignin and additionally saturate the aromatic rings [17–19]. Selective oxidation does not have these deficiencies and is a method to convert lignin and maintain the aromatic rings [20, 21].

Recently, advanced selective oxidation has been investigated extensively, and various homogeneous and heterogeneous transition metal catalysts have been used in the oxidation of lignin and lignin models, including cobalt [22–24],

**Highlights** MeCN/H<sub>2</sub>O was developed as the medium for oxovanadium catalyzed lignin oxidation.

Oxovanadium complexes can effectively cleave lignin linkages in MeCN/H<sub>2</sub>O under O<sub>2</sub>.

Vanadium valence changes during lignin oxidation were verified by EPR and <sup>51</sup>V NMR.

Phenolic product-induced condensation during lignin oxidation was confirmed by LC-MS.

✉ Rui Xiao  
ruixiao@seu.edu.cn

<sup>1</sup> Key Laboratory of Energy Thermal Conversion and Control of Ministry of Education, School of Energy and Environment, Southeast University, Nanjing 210096, China

copper [25–29], vanadium [27, 28, 30–32], and other species [11, 33–35]. Since Son and Toste [30] found the high catalytic activity of oxovanadium complexes in lignin model conversion, oxovanadium complexes catalyzed oxidation quickly became a research hotspot. Afterwards, Hanson et al. [31] reported that the selectivity of oxovanadium catalysts depended on their ligands. With a theoretical study, Jiang et al. [36] further derived the detailed catalytic degradation mechanism of oxovanadium catalysts with different ligands. Various homogeneous oxovanadium complexes were developed for lignin and lignin model oxidations with O<sub>2</sub>/air [37–39]. However, among these reported oxovanadium complexes catalyzed oxidations, yields of phenolic products, e.g., phenol or guaiacol, were lower than the yields of synchronization substances (aromatic aldehydes and/or acids) and dimer conversion [27, 28].

Previous studies have shown that the solvent system has an important influence on catalyst performance. A solvent should be able to coordinate with the catalyst and enhance lignin oxidation degradation. At present, pyridine is often employed as the solvent for oxovanadium complexes catalyzed oxidation of lignin and lignin dimers [27, 32, 37, 38], whose coordination with oxovanadium catalysts has been systematically investigated by Hanson et al. [40]. However, pyridine is toxic to the human body and environment. Therefore, developing new and efficient solvents is important for developing lignin catalytic oxidation reactions. Acetic acid, acetonitrile (MeCN), triethylamine, toluene, and dimethyl sulfoxide were developed as solvents for lignin and lignin dimer oxidation and exhibited good performances [28, 32, 37, 39]. Here, we reported a new oxidation solvent system, MeCN/H<sub>2</sub>O co-solvents, which with oxovanadium catalysts selectively converted lignin dimers. Meanwhile, we investigated the catalytic oxidation of phenolic products (including phenol, guaiacol, and syringol), and revealed undesired repolymerization reactions. This system was also applied to the oxidation of poplar organosolv lignin.

## 2 Experimental section

### 2.1 Materials and chemicals

Lignin dimers were synthesized according to the literature procedures [41]. Their synthesis schemes, as well as structure identification with <sup>1</sup>H and <sup>13</sup>C NMR were displayed in Figs. S1–S5. Lignin sample used in this study was poplar organosolv lignin. It was prepared with the published method [42]. Vanadyl<sup>IV</sup> acetylacetonate (VO(acac)<sub>2</sub>, 99%) and vanadium<sup>III</sup> acetylacetonate (V(acac)<sub>3</sub>, 98%) were purchased from J&K scientific Ltd (Beijing, China). Acetonitrile (MeCN, HPLC grade), tetrahydrofuran (THF, HPLC grade), *n*-dodecane (standard for GC, ≥ 99.5%), diethyl

ether (Et<sub>2</sub>O, AR grade), and deuterated dimethyl sulfoxide (DMSO-*d*<sub>6</sub>) were all commercially available and used as received. Deionized water was produced in our lab. High purity O<sub>2</sub> was provided by Nanjing Shangyuan Gas Company (Nanjing, China).

### 2.2 General procedure for catalytic oxidation of lignin models

Lignin models (0.25 mmol) were separately charged into a 25 mL batch reactor, together with the catalyst (VO(acac)<sub>2</sub> or V(acac)<sub>3</sub>, 10 mol%), and a magnetic stirrer. Subsequently, MeCN/H<sub>2</sub>O co-solvent (15 mL, v/v) was added. The reactor was purged three times with oxygen and charged with 1.5 MPa of oxygen, and the reaction mixture was stirred at 1000 rpm at 140 °C. After the desired reaction time, the reactor was quenched with ice water. The remaining oxygen pressure was released, and the reactor was opened. The mixture was first filtered to remove residues, and then evaporated under reduced pressure to remove solvent. To quantify produced monomeric products, 2 mL standard solution (*n*-dodecane in THF, 0.02 mol/L) was added to dissolve the concentrated mixture. Then, the sample was detected using GC–MS and GC–FID. Schematic procedure for lignin model oxidation was illustrated in Fig. S6.

### 2.3 General procedure for catalytic oxidation of lignin

Lignin powder (0.2 g) was charged into a 50 mL batch reactor, together with the VO(acac)<sub>2</sub> catalyst (15 wt.%), and a magnetic stirrer. Subsequently, MeCN/H<sub>2</sub>O co-solvent (30 mL, 1:1, v/v) was added. The reactor was purged three times with oxygen and charged with 1.5 MPa of oxygen, and the reaction mixture was stirred at 1000 rpm at 140 °C for 48 h. After reaction, the reactor was quenched with ice water. The remaining oxygen pressure was released, and the reactor was opened. The mixture was first filtered to remove residues, and then evaporated under reduced pressure to remove solvent. Then, the concentrated mixture was added dropwise to Et<sub>2</sub>O to precipitate unreacted feed and produced oligomers. Next, the precipitate was centrifugated, washed three times with Et<sub>2</sub>O, and dried. Part of the obtained solid residue was dissolved with DMSO-*d*<sub>6</sub> to identify the lignin structure evolution using 2D HSQC NMR. The other part of the precipitate was further acetylated [43, 44], and then dissolved in THF (HPLC grade) to analyze the molecular weight changes using GPC. Schematic procedure for lignin oxidation was illustrated in Fig. S7.

## 2.4 Products analysis and data processing

Products from lignin model oxidation were qualitatively analyzed by GC–MS using an Agilent 7890B gas chromatograph and an Agilent 5977B mass spectrometer equipped with an HP-INNOWAX capillary column. The injection temperature was 260 °C. 1  $\mu$ L of sample was injected with an autosampler in split mode (split ratio 30:1). The column temperature was programmed from 50 °C (2 min) to 250 °C (10 min) with a heating rate of 6 °C/min. The mass spectrometer was set at an ionizing voltage of 70 eV, and the mass range was scanned from  $m/z$  33 to 400. The products were identified by comparing the MS spectra with standard compounds.

Then, monomers generated after oxidation were quantified on a GC-2014 (Shimadzu, Japan) with an HP-INNOWAX capillary column and a flame ionization detector (FID). For GC-FID, the split ratio was 10:1, and the temperature program started from 50 °C holding for 2 min, and then raised to 250 °C holding for 33 min with a heating rate of 6 °C/min. Product yields were calculated based on the effective carbon number (ECN) as described in the literature [45], in which the ECNs of monomers and reactants were corrected with the standard compounds in THF. Specific calculation formulae for substrate conversion and monomer yield can be found in Eqs. (1) and (2), respectively.

$$C(\text{mol}\%) = \frac{n_{\text{initial}} - n_{\text{final}}}{n_{\text{initial}}} \times 100\% \quad (1)$$

$$Y_i(\text{mol}\%) = \frac{n_i}{n_{\text{initial}}} \times 100\% \quad (2)$$

where  $C$  represented the conversion of substrate,  $Y_i$  was the mole yield of product  $i$ ,  $n_{\text{initial}}$  and  $n_{\text{final}}$  were separately the mole of substrate before and after reaction, and  $n_i$  was the mole of product  $i$ .

Oligomers generated from lignin dimer and phenolic reactant oxidation were characterized using a liquid chromatograph coupled with a mass spectrometer (LC–MS, 1290 Infinity LC/6460 QQQ MS, Agilent Technologies, USA) equipped with an electrospray ionization (ESI) source working in the positive mode. Nitrogen was used as the nebulizer gas with a flow volume of 10.0 L/min and a nebulizer pressure of 45 psi. The nozzle and capillary voltage were separately set at 500 and 3500 V. The mass range was from  $m/z$  100 to 1000.

Oxovanadium complexes before and after oxidation were conducted using EPR and  $^{51}\text{V}$  NMR. EPR spectra were recorded on a Bruker EMX-10/12 instrument operating at approximately 9.77 GHz (X-band) at room temperature.  $^{51}\text{V}$  NMR spectra were carried out on a Bruker AVIII 600 NMR spectrometer at room temperature. HSQC NMR and GPC

characterizations of poplar organosolv lignin and its heavy fractionation were performed as described in our previous report [43].

## 3 Results and discussion

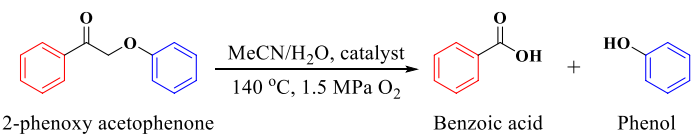
### 3.1 Oxovanadium complexes catalyzed oxidation of lignin dimer 1a in MeCN/H<sub>2</sub>O

VO(acac)<sub>2</sub> and ketone-structure lignin model 2-phenoxy acetophenone (dimer 1a) were selected as the catalyst and reactant to investigate catalytic oxidation in MeCN and MeCN/H<sub>2</sub>O co-solvent systems (Entries 1–9, Table 1). After a VO(acac)<sub>2</sub> catalyzed oxidation for 8 h in MeCN, there was only 17 mol% conversion of dimer 1a (Entry 1, Table 1). Correspondingly, the yields of phenol and benzoic acid were both quite low, separately 2 mol% and 5 mol%. Interestingly, when we changed the reaction solvent from pure MeCN to MeCN/H<sub>2</sub>O co-solvent (1:1, v/v), the conversion increased to 44 mol% with product yields of 26 mol% and 38 mol% respectively (Entry 2, Table 1). The active site of homogeneous VO(acac)<sub>2</sub> catalyst comes from the vanadium<sup>IV</sup> center. Meanwhile, VO(acac)<sub>2</sub> has Lewis acid sites, so the added water promoted its hydrolysis to expose the vanadium<sup>IV</sup> center more easily, increasing catalytic activity[46].

The MeCN/H<sub>2</sub>O co-solvent system was optimized to obtain higher dimer conversion and product yields (Entries 2–5, Table 1). By extending the reaction time from 8 to 24 h, the dimer conversion increased from 44 mol% to 95 mol%. The yields of phenol and benzoic acid increased from 26 mol% and 38 mol% to 43 mol% and 83 mol% respectively. In this reaction system, the benzoic acid and phenol yields were always lower than the dimer conversion with the phenol yield around half of benzoic acid yield. The low phenol yield during lignin model oxidation is commonly reported in literatures [27, 28]. The investigation and explanation of these phenomena would be discussed subsequently.

The solvent ratio of MeCN to H<sub>2</sub>O is also an important factor that can influence dimer conversion and product yields. We optimized the MeCN/H<sub>2</sub>O ratio from 1:0 to 1:3 to determine the optimal solvent ratio (Entries 5–8, Table 1). The conversion of dimer 1a increased from 44 mol% to 67 mol%, then to 95 mol%, and finally achieved 100 mol% with adjusting the MeCN/H<sub>2</sub>O ratios from 1:0 to 3:1, 1:1, and 1:3. Consistent with the improved conversion, the product yields increased, and reached the maximums when the MeCN/H<sub>2</sub>O ratio was fixed at 1:1. Whereafter, the MeCN/H<sub>2</sub>O ratio became 1:3, but the product yields dropped to 4 mol% (phenol) and 60 mol% (benzoic acid) (Entry 8, Table 1). This suggested that the proper MeCN/H<sub>2</sub>O ratio (1:1, v/v) can favor the VO(acac)<sub>2</sub> hydrolysis, as well as

**Table 1** Optimization of reaction conditions of oxidative cleavage of 2-phenoxy acetophenone ( $\beta$ -O-4 lignin dimer 1a)<sup>[a]</sup>



2-phenoxy acetophenone  $\xrightarrow[140\text{ }^\circ\text{C, 1.5 MPa O}_2]{\text{MeCN/H}_2\text{O, catalyst}}$  Benzoic acid + Phenol

Entry	Catalyst	MeCN/H <sub>2</sub> O (v/v)	Time (h)	Conversion (mol%) <sup>[b]</sup>	Yield (mol%) <sup>[b]</sup>	
					Phenol	Benzoic acid
1	VO(acac) <sub>2</sub>	1:0	8	17	2	5
2	VO(acac) <sub>2</sub>	1:1	8	44	26	38
3	VO(acac) <sub>2</sub>	1:1	12	62	32	50
4	VO(acac) <sub>2</sub>	1:1	16	76	37	60
5	VO(acac) <sub>2</sub>	1:1	24	95	43	83
6	VO(acac) <sub>2</sub>	1:0	24	44	3	23
7	VO(acac) <sub>2</sub>	3:1	24	67	26	42
8	VO(acac) <sub>2</sub>	1:3	24	100	4	60
9 <sup>[c]</sup>	VO(acac) <sub>2</sub>	1:1	24	66	16	42
10	V(acac) <sub>3</sub>	1:0	24	16	>1	10
11	V(acac) <sub>3</sub>	3:1	24	96	13	70
12	V(acac) <sub>3</sub>	1:1	24	100	13	77
13	V(acac) <sub>3</sub>	1:3	24	100	11	69
14	V(acac) <sub>3</sub>	1:1	16	87	25	62
15	V(acac) <sub>3</sub>	1:1	8	56	27	38

<sup>[a]</sup>Reaction conditions: lignin dimer 1a (0.25 mmol), catalyst (10 mol%), O<sub>2</sub> (1.5 MPa), solvent (15 mL), 140 °C, stirring rate 1000 rpm. <sup>[b]</sup>Conversions and yields were determined by GC-FID with *n*-dodecane as the internal standard. <sup>[c]</sup>Air (1.5 MPa) instead of O<sub>2</sub>.

promote the dimer conversion and product yields, but too much water leads to the degradation of products.

The role of oxygen partial pressure was also explored in Entry 9 (Table 1). Replacing pure oxygen with air, the conversion efficiency of dimer 1a decreased from 95 mol% to 66 mol%, and the yields of phenol and benzoic acid lowered from 43 mol% to 16 mol% and from 83 mol% to 42 mol%, respectively. These data illustrated that oxygen pressure

influenced the dimer conversion and product yields. Oxygen is involved in our reaction, similar to other oxovanadium complexes catalyzed aerobic oxidation [31, 36]. However, main products in our system and literatures were quite different. The oxidative products in literatures were benzoquinone [31, 36], whereas our dominant product was benzoic acid. This difference should be caused by the different oxidation mechanism. At this moment, we summarized the optimized

conditions for  $\text{VO}(\text{acac})_2$  catalyzed dimer 1a conversion which were at 140 °C for 24 h under 1.5 MPa  $\text{O}_2$  pressure in  $\text{MeCN}/\text{H}_2\text{O}$  co-solvent (1:1, v/v).

$\text{V}(\text{acac})_3$ , the homogenous vanadium<sup>III</sup> catalyst, for lignin oxidation was also studied [27]. So, it was further employed for lignin dimer oxidation as a contrast in our  $\text{MeCN}/\text{H}_2\text{O}$  co-solvent system (Entries 10–15, Table 1). With  $\text{V}(\text{acac})_3$ ,  $\text{MeCN}/\text{H}_2\text{O}$  ratios also influenced the conversion of dimer 1a and the yields of phenol and benzoic acid (Entries 10–13, Table 1). Lower  $\text{MeCN}/\text{H}_2\text{O}$  ratios increased the dimer 1a conversion from 16 mol% to 100 mol%. When the  $\text{MeCN}/\text{H}_2\text{O}$  ratio was 1:1, the optimal yields of phenol (13 mol%) and benzoic acid (77 mol%) were achieved. However, these two yields were lower than the optimized results of  $\text{VO}(\text{acac})_2$  catalyzed oxidation (43 mol% and 83 mol%, Entry 5, Table 1). In order to present the catalytic effects of  $\text{VO}(\text{acac})_2$  and  $\text{V}(\text{acac})_3$  in our  $\text{MeCN}/\text{H}_2\text{O}$  system, we did another two reactions using  $\text{V}(\text{acac})_3$  with 16 h and 8 h respectively, as listed in Entries 14 and 15 (Table 1), and compared them with the results from  $\text{VO}(\text{acac})_2$  under the same reaction conditions (Entries 4 and 2, Table 1). As shown in these three comparison groups (8 h, 16 h, and 24 h), the dimer 1a conversions with  $\text{V}(\text{acac})_3$  were higher than those with  $\text{VO}(\text{acac})_2$  (56 mol% vs. 44 mol%, 87 mol% vs. 76 mol%, and 100 mol% vs. 95 mol%), but the corresponding yields were similar to or lower than those with  $\text{VO}(\text{acac})_2$  (27 mol% vs. 26 mol%, 25 mol% vs. 37 mol%, and 13 mol% vs. 43 mol% for phenol; 38 mol% vs. 38 mol%, 62 mol% vs. 60 mol%, and 77 mol% vs. 83 mol% for benzoic acid). All these directly indicated that the catalytic oxidative activity of  $\text{V}(\text{acac})_3$  in  $\text{MeCN}/\text{H}_2\text{O}$  system (1:1, v/v) was

higher than that of  $\text{VO}(\text{acac})_3$ , but the repolymerization was higher. In the following, we explored the details of catalytic oxidation with ESI–MS, EPR, and  $^{51}\text{V}$  NMR.

As analyzed above, both oxovanadium complexes had lower than 100% selectivity to known products. Even for the optimal conditions of  $\text{VO}(\text{acac})_2$  (Entry 5, Table 1), there were still big gaps between the yields of phenol (43 mol%) and benzoic acid (83 mol%) which should be produced in equal molar amounts. To understand these side reactions, we analyzed the reaction mixtures after 24 h using ESI–MS. ESI–MS can identify the soluble high molecular weight fragments which cannot be detected in GC–MS and GC–FID. As presented in Fig. 1, the ESI–MS was set at the positive mode and recorded the molecular weight of  $[\text{M} + \text{Na}]^+$  or  $[\text{M} + \text{H}]^+$  species. The  $m/z$  235 specie (212 Da) was the react dimer while the  $m/z$  447 specie (424 Da) (likely the bimolecular complex), and other high  $m/z$  fragments directly indicated the condensation reactions in dimer 1a oxidation. Furthermore, the intensity of high molecular weight fragments in  $\text{V}(\text{acac})_3$  catalyzed system (Fig. 1b) was higher than those in  $\text{VO}(\text{acac})_2$  (Fig. 1a). That was to say repolymerization in  $\text{V}(\text{acac})_3$  catalyzed oxidation was more prevalent than that of  $\text{VO}(\text{acac})_2$  system, corresponding to the lower product yields catalyzed by  $\text{V}(\text{acac})_3$ . Considering the possible conversion routes of dimer 1a, we thought the coupling product was the phenol.

We further focused on the catalysts, and performed EPR and  $^{51}\text{V}$  NMR of  $\text{VO}(\text{acac})_2$  and  $\text{V}(\text{acac})_3$  before and after dimer 1a oxidation (Fig. 2). The EPR technique gives the signals of single electrons, so it can detect the existence of vanadium<sup>IV</sup> species [47]. As depicted in Fig. 2a. The EPR

**Fig. 1** ESI–MS spectra of reaction mixtures after  $\text{VO}(\text{acac})_2$  (a) and  $\text{V}(\text{acac})_3$  (b) catalyzed oxidation. Reaction conditions: lignin model 1a (0.25 mmol), catalyst (10 mol%),  $\text{O}_2$  (1.5 MPa),  $\text{MeCN}/\text{H}_2\text{O}$  co-solvent (15 mL, 1:1, v/v), 140 °C, 24 h, stirring rate 1000 rpm

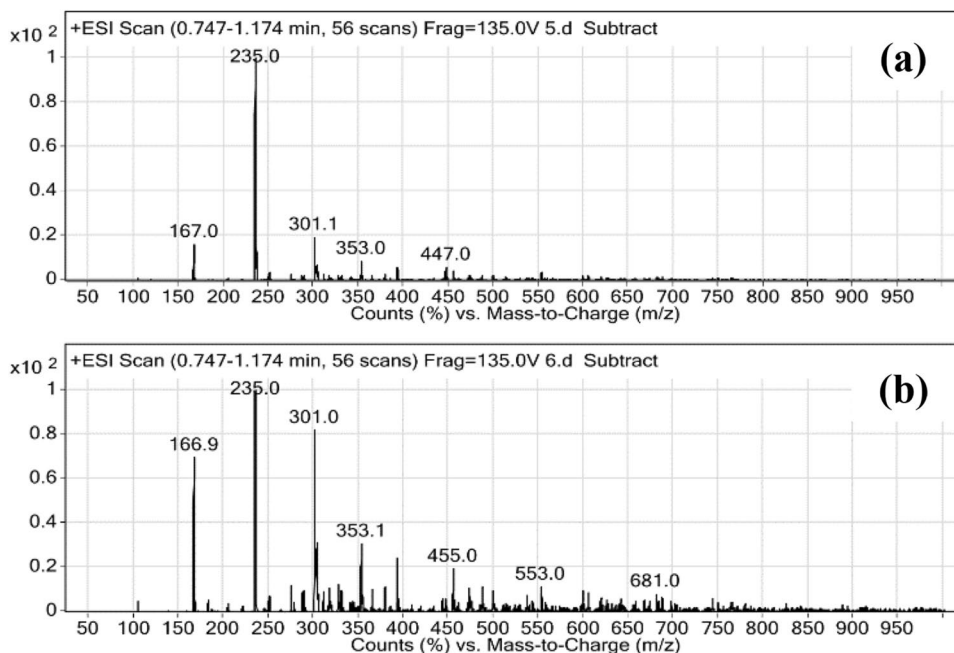
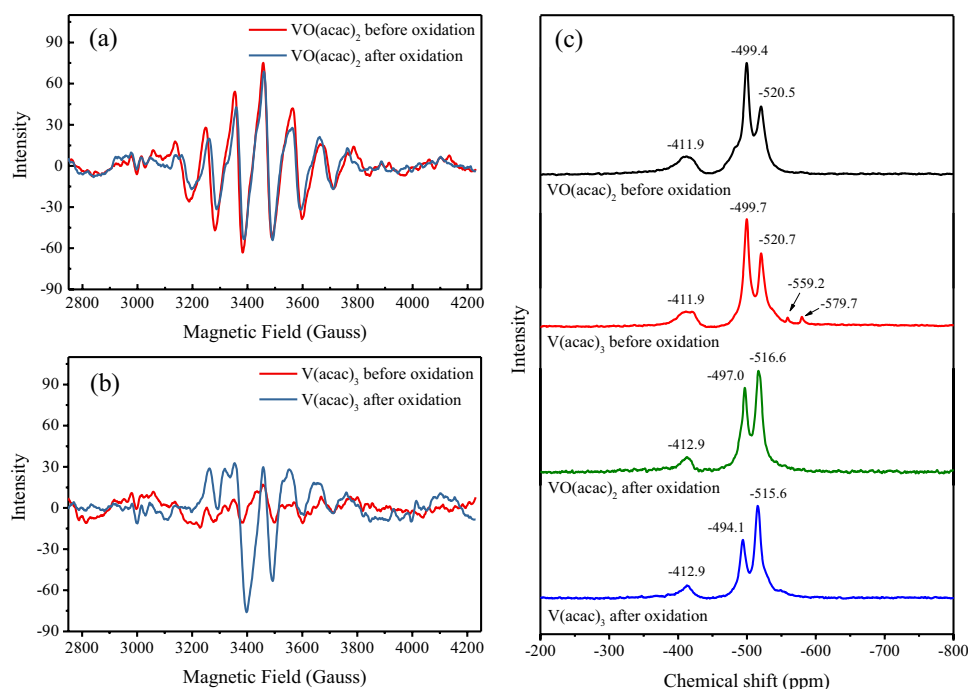


**Fig. 2** EPR (a and b) and  $^{51}\text{V}$  NMR (c) spectra of  $\text{VO}(\text{acac})_2$  and  $\text{V}(\text{acac})_3$  before and after lignin model 1a oxidation. Reaction conditions: lignin model 1a (0.25 mmol), catalyst (10 mol%),  $\text{O}_2$  (1.5 MPa),  $\text{MeCN}/\text{H}_2\text{O}$  co-solvent (15 mL, 1:1, v/v), 140 °C, 24 h, stirring rate 1000 rpm



signals of  $\text{VO}(\text{acac})_2$  before and after oxidation were both the typical signals of vanadium<sup>IV</sup> center, but the intensity of  $\text{VO}(\text{acac})_2$  after oxidation was slightly weaker than that of  $\text{VO}(\text{acac})_2$  before oxidation. This roughly indicated that the main part of  $\text{VO}(\text{acac})_2$  after oxidation was kept, but the small part was transformed. Wehrli and Stumm reported that  $\text{VO}(\text{acac})_2$  can transform to  $\text{VO}^{2+}$  in  $\text{H}_2\text{O}$ , and the generated  $\text{VO}^{2+}$  would combine with  $\text{O}_2$  together with  $\text{H}_2\text{O}$  to form various O-VO complexes [46]. Additionally, during these reactions, the valence of vanadium<sup>IV</sup> changes, and possibly caused the EPR signal to decrease after oxidation. The EPR signal of  $\text{V}(\text{acac})_3$  before oxidation was noisy, but several peaks of typical vanadium<sup>IV</sup> signals can still be recognized (Fig. 2b). Theoretically,  $\text{V}(\text{acac})_3$  has no EPR signals, thus these weak signals suggested the existence of vanadium<sup>IV</sup> center, and its concentration was quite low. The vanadium<sup>IV</sup> center should be produced from the oxidation of  $\text{V}(\text{acac})_3$ , even though  $\text{O}_2$  was only charged before reaction (see the sampling process in Fig. S6). After oxidation, the intensity of EPR signals became stronger. This reflected the increase of vanadium<sup>IV</sup> concentration in  $\text{V}(\text{acac})_3$  catalyzed system after oxidation and revealed the transformation from vanadium<sup>III</sup> to vanadium<sup>IV</sup> under  $\text{O}_2$  in  $\text{MeCN}/\text{H}_2\text{O}$ . Furthermore, a couple of peaks were split, and two peaks around 3400 G and 3500 G were markedly strengthened (Fig. 2b). These phenomena were different with those of  $\text{VO}(\text{acac})_2$  after oxidation and suggested the interference in  $\text{V}(\text{acac})_3$  catalyzed system after oxidation. Compared with the EPR signals of various oxovanadium complexes [48–50], our peak shape was different. That was because EPR samples used in previous works were pure organic oxovanadium

complexes dissolved in solvent. But our samples were collected from reaction systems, where they were mixed with reactant, and/or products, and charged with  $\text{O}_2$ . Literatures also displayed that the EPR signals of the same oxovanadium complexes were different in various solvents [51]. Therefore, all these might lead to the difference of our EPR signals.

To comprehensively describe the changes of  $\text{VO}(\text{acac})_2$  and  $\text{V}(\text{acac})_3$  before and after oxidation, we further employed  $^{51}\text{V}$  NMR to monitor the emergence of vanadium<sup>V</sup> [32, 47, 52–54], and the corresponding spectra were illustrated in Fig. 2c. Before oxidation, signals of vanadium<sup>V</sup> were observed in both  $\text{VO}(\text{acac})_2$  and  $\text{V}(\text{acac})_3$  catalyzed solutions. That meant  $\text{VO}(\text{acac})_2$  and  $\text{V}(\text{acac})_3$  can react with  $\text{O}_2$  quickly, forming  $\text{V}^{\text{V}}\text{-O}$  complexes. Furthermore,  $^{51}\text{V}$  NMR signals from these two solutions were similar, except for two small peaks at  $-559.2$  ppm and  $-579.7$  ppm. This suggested that similar vanadium<sup>V</sup> species were formed from  $\text{VO}(\text{acac})_2$  and  $\text{V}(\text{acac})_3$  after charging  $\text{O}_2$ . After reaction, the vanadium<sup>V</sup> signals from both  $\text{VO}(\text{acac})_2$  and  $\text{V}(\text{acac})_3$  were still similar, indicating almost the same vanadium<sup>V</sup> species after oxidation. However, the chemical shifts, as well as the relative intensities of these vanadium<sup>V</sup> signals after oxidation changed as compared with those before oxidation. This meant the different vanadium<sup>V</sup> species existence before and after oxidation. Together with the results of EPR, we can conclude that during dimer 1a oxidation, a portion of  $\text{VO}(\text{acac})_2$  was converted to vanadium<sup>V</sup> species, while a portion of  $\text{V}(\text{acac})_3$  was transformed to vanadium<sup>IV</sup> and vanadium<sup>V</sup> species. The active site for both  $\text{VO}(\text{acac})_2$  and  $\text{V}(\text{acac})_3$  catalysts should be the same generated V–O complexes, containing vanadium<sup>IV</sup> and vanadium<sup>V</sup> center.

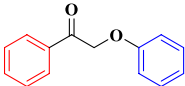
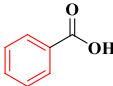
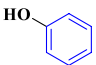
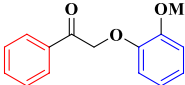
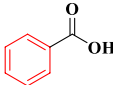
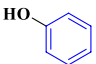
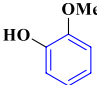
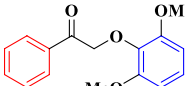
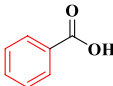
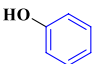
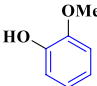
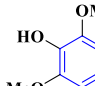
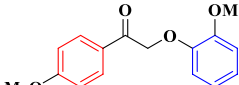
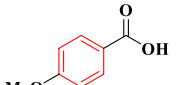
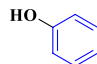
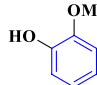
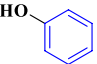
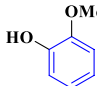
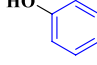
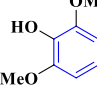
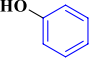
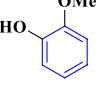
However, the exact structures of these vanadium species were hard to identify. In general, owing to the higher monomer yields and lower repolymerization, we chose VO(acac)<sub>2</sub> for all of the subsequent oxidations with MeCN/H<sub>2</sub>O co-solvent.

### 3.2 VO(acac)<sub>2</sub> catalyzed oxidation of various lignin models in MeCN/H<sub>2</sub>O

Three β-O-4 lignin dimers were further employed to verify the catalytic oxidation ability of VO(acac)<sub>2</sub> in MeCN/H<sub>2</sub>O system under O<sub>2</sub>. The conversions, as well as the yields of various products under optimized conditions were

summarized in Entries 1–4, Table 2. As discussed above, the highest conversion of dimer 1a was 95 mol% (Entry 5 in Table 1). After replacing the subspecies in lignin dimers from phenol (1a) to guaiacol (1b) and syringol (1c), as well as from acetophenone (1a) to *p*-methoxy acetophenone (1d), the conversions were similar, and were all higher than 95 mol%. This results illustrated the high catalytic ability of VO(acac)<sub>2</sub> for various β-O-4 lignin dimers oxidation. Enhanced conversion was observed from the addition of OMe groups. The promoting role of the OMe group is widely observed in lignin and lignin dimer conversion [33, 55–57]. The OMe group has not only the spatial effect but also the electron donating effect. These two effects could

**Table 2** Oxidation of various lignin models with VO(acac)<sub>2</sub> catalyst<sup>[a]</sup>

Entry	Substrate, conversion (mol%)	Products, yields (mol%)
1	 1a, 95 mol%	 +  2a, 83 mol%    3a, 43 mol%
2	 1b, 98 mol%	 +  +  2a, 73 mol%    3a, 3 mol%    3b, trace
3	 1c, >99 mol%	 +  +  +  2a, 64 mol%    3a, 3 mol%    3b, <2 mol%    3c, <1 mol%
4	 1d, 97 mol%	 +  +  2b, 65 mol%    3a, <1 mol%    3b, trace
5	 3a, 65 mol%	No GC detected products
6	 3b, ~100 mol%	 3a, >11 mol%
7	 3c, ~100 mol%	 +  3a, <3 mol%    3b, trace

<sup>[a]</sup>Reaction conditions: substrate (0.25 mmol), VO(acac)<sub>2</sub> (10 mol%), O<sub>2</sub> (1.5 MPa), MeCN/H<sub>2</sub>O co-solvent (15 mL, 1:1, v/v), 140 °C, 24 h (Entries 1–4) or 8 h (Entries 5–7), stirring rate 1000 rpm. Conversions and yields were determined by GC-FID with *n*-dodecane as the internal standard.

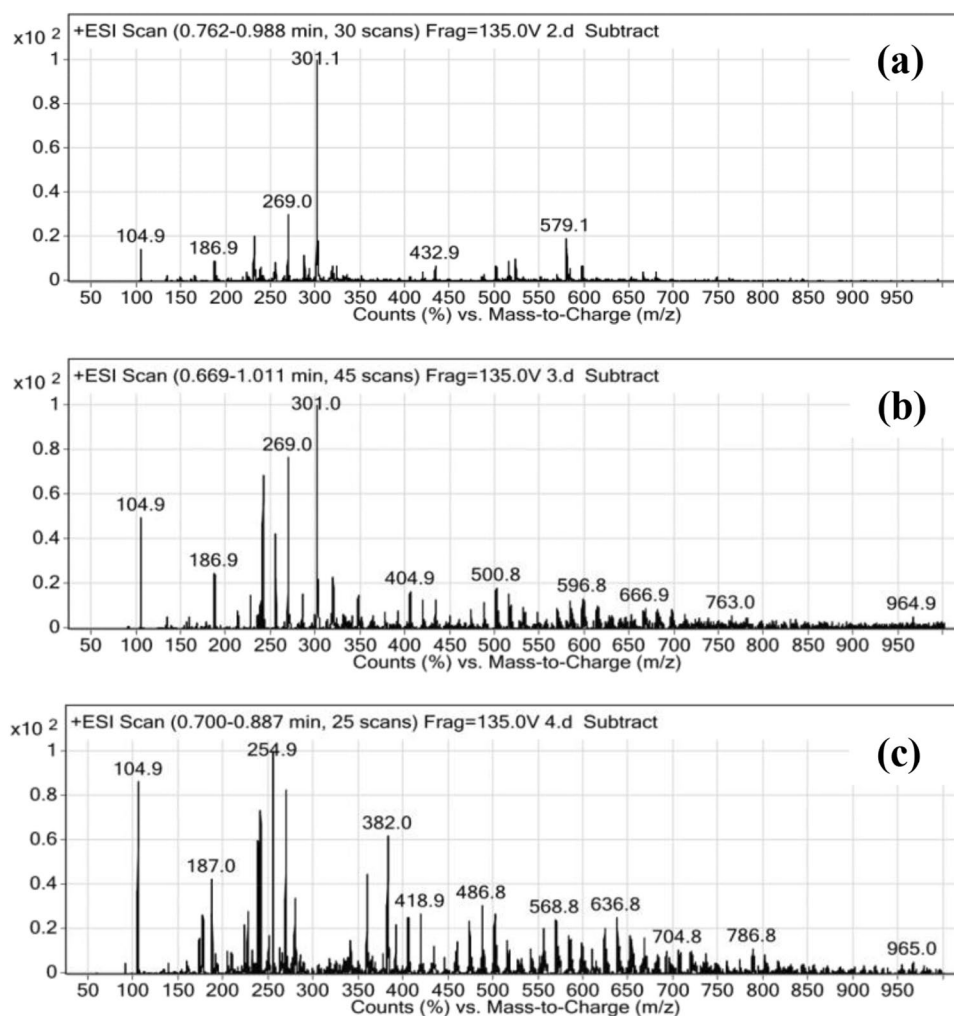
both lead the  $\beta$ -O-4 linkage weak, i.e., lower the bond dissociation energy, and make it easy to be broken [58].

Oxidation products from the four lignin dimers were benzoic acid 2a (or *p*-methoxy benzoic acid 2b), and phenolic compounds (including phenol 3a, guaiacol 3b, and syringol 3c). In contrast with the dimer conversion favored by the OMe group, the yields of all products decreased. The 2a yield from 1a conversion was 83 mol%, but it decreased to 73 mol% in 1b conversion, and then went on to 64 mol% in 1c conversion (Table 2). For 1d oxidation, the corresponding 2b yield was 65 mol%, similar with the 2a yield in 1c conversion. As presented in Table 2, the phenol 3a yield from 1a conversion was 43 mol%. However, in the conversion of 1b and 1c, the 3a yield was only 3 mol%. Though, guaiacol 3b and syringol 3c were also the detectable products in these two dimers, their yields were low (Entries 2 and 3, Table 2). Among the phenolic compounds from 1d oxidation, only less than 1 mol% yield of 3a and trace amount of 3b were observed (Entry 4, Table 2), which were markedly lower than the phenolic yields. The slight drop of product yields might be ascribed to the different molecular structures

of lignin dimers. However, the yield decrease should not be only caused by the dimer molecular structure changes, other reactions should also occur, such as degradation or condensation.

In order to further confirm the secondary reactions (especially condensation) of oxidation products, mainly the phenolic species, we directly used phenolic compounds (phenol, guaiacol, and syringol) as the reactants to do the oxidation. Conversions of phenolic compound and the corresponding yields of products were summarized in Entries 5–7, Table 2. Meanwhile, the molecular weight distributions of produced oligomers verified with ESI-MS were displayed in Fig. 3. After phenol oxidation for 8 h, 65 mol% conversion was observed, but no products were detected by GC-MS and GC-FID (Entry 5, Table 2). As for guaiacol, its oxidation conversion was close to 100 mol%, and the only identified product was phenol, with the yield of > 11 mol%. Syringol underwent the most serious oxidation. Its conversion was also nearly complete, whereas less than 3 mol% phenol and trace guaiacol were produced. Except for the reactant itself and the demethoxylated products, no other monomers were

**Fig. 3** ESI-MS spectra of reaction mixtures from phenol (a), guaiacol (b), and syringol (c) oxidation. Reaction conditions: substrate (0.25 mmol), VO(acac)<sub>2</sub> (10 mol%), O<sub>2</sub> (1.5 MPa), MeCN/H<sub>2</sub>O co-solvent (15 mL, 1:1, v/v), 140 °C, 8 h, stirring rate 1000 rpm





observed in the reaction mixtures. We suspected the missing reactants converted to the unknown fragments with high molecular weight that cannot be detected with GC–MS and GC–FID. So, we further employed ESI–MS to identify those high molecular weight fragments.

ESI–MS for phenolic oxidation product identification was also set at the positive mode. In these ESI–MS spectra (Fig. 3), some fragments with the same molecular weight were observed, such as  $m/z$  105, 187, 169, 301, and so on. This mainly attributed to the same main structure of three phenolic reactants. Guaiacol and syringol are both methoxylated phenols, so they can produce products with the similar molecular weights. Among these phenolic reactants, phenol underwent the lowest condensation. It only had several high molecular weight fragments, including  $m/z$  433, 523, and 579 (Fig. 3a). Condensation during guaiacol oxidation was heavier than that occurred in phenol oxidation. As Fig. 3b illustrated, more high molecular weight fragments were detected, and their intensities were also higher than those in phenol oxidation. Large amounts of high molecular weight fragments existed in the reaction mixture after syringol oxidation (Fig. 3c). Combined with its lowest monomer yields (Entry 7, Table 2), we can easily conclude that syringol had the heaviest condensation during VO(acac)<sub>2</sub> catalyzed oxidation. The structural difference between phenol, guaiacol, and syringol is the OMe groups, thus the heavier condensation during guaiacol and syringol oxidation should be caused by the OMe group. That meant OMe group promoted the condensation reactions. In oxidation system, phenolic OH group can be transformed to phenoxy radical. This radical can couple to C<sub>2</sub>, C<sub>4</sub>, or C<sub>6</sub> position easily, leading to the condensation to unknown compounds with high molecular weight, as illustrated in Fig. S8 [59]. That was the reason why phenolics were unstable in oxidative conditions. Furthermore, the OMe group in guaiacol and syringol can donate electron to the benzene ring and accelerate the oxidation condensation reactions. However, the detailed pathways to form these oligomers in our system were still unknown. Based on the above analysis, we can explain why dimer 1a had the highest product yields, followed by dimer 1b, and the product yields from dimer 1c and 1d were the lowest (Entries 1–4, Table 2). During VO(acac)<sub>2</sub> catalyzed aerobic oxidation of lignin dimers, the phenol product (guaiacol or syringol) underwent further oxidation. They would couple with not only other phenolic fragments but also benzoic acid (or *p*-methoxy benzoic acid).

### 3.3 VO(acac)<sub>2</sub> catalyzed oxidation of lignin in MeCN/H<sub>2</sub>O

We demonstrated the catalytic effect of VO(acac)<sub>2</sub> on lignin dimer oxidation in MeCN/H<sub>2</sub>O system under O<sub>2</sub>. Here we applied this reaction system into real lignin oxidation. To

evaluate the degree of oxidative depolymerization of poplar organosolv lignin, we elucidated the structure with NMR and the molecular weight changes with GPC. HSQC NMR is an advanced technique in lignin structural analysis, and it is also widely used in lignin depolymerization analyses [43, 60–64]. That is because HSQC NMR can give specific <sup>13</sup>C–<sup>1</sup>H correlations, however these signals might be overlapped in cluttered <sup>13</sup>C and <sup>1</sup>H spectra [43, 63]. Moreover, HSQC NMR can give relative quantities or semi-quantitative results of aromatic units and C–O linkages within lignin fractionations, which provides semi-quantification of lignin structure evolution [43, 61, 64].

The HSQC NMR spectra of poplar organosolv lignin and its heavy fractionation after VO(acac)<sub>2</sub> catalyzed oxidation were illustrated in Fig. 4, including C–O aliphatic ( $\delta_H/\delta_C$  3.0–6.0/50–90) and aromatic ( $\delta_H/\delta_C$  6.0–8.0/100–140) functionalities. These chemical shifts of identified peaks were determined according to literatures [43, 60, 63–66] and summarized in Table S1. In C–O aliphatic region of poplar organosolv lignin (Fig. 4a), cross-signals of the OMe groups,  $\beta$ -O-4 aryl ether linkages (A), C <sub>$\gamma$</sub> -acetylated  $\beta$ -O-4 aryl ether linkages (A'), resinol substructures formed by  $\beta$ - $\beta$ ,  $\alpha$ -O- $\gamma$  and  $\gamma$ -O- $\alpha$  linkages (B), and phenylcoumarane substructures formed by  $\beta$ -5 and  $\alpha$ -O-4 linkages (C) were all clearly recognized. Peaks of A' <sub>$\alpha$</sub>  ( $\delta_H/\delta_C$  5.93/74.5 for *Erythro* and  $\delta_H/\delta_C$  6.00/74.8 for *Threo*) and A' <sub>$\beta$</sub>  ( $\delta_H/\delta_C$  4.57/80.6) were resulted from the acetylation during lignin preparation [60] owing to the existence of acetic acid. The quantities of  $\beta$ -O-4,  $\beta$ - $\beta$ , and  $\beta$ -5 linkages within poplar organosolv lignin were separately 34.0, 3.1, and 3.9 (based on per 100 Ar [43, 65, 67]). The high frequency of  $\beta$ -O-4 linkages suggested the easy degradability of poplar organosolv lignin. After oxidation, apart from the signals of OMe groups and remaining A <sub>$\gamma$</sub> , no other signals of C–O aliphatic linkages were observed in the heavy fractionation (Fig. 2b). This did reflect the oxidative degradation of poplar organosolv lignin, and all ether bonds with lignin molecule were cleaved. The degree of degradation would be measured by GPC and discussed in the following parts.

In aromatic region of poplar organosolv lignin (Fig. 4a), cross-signals from the syringyl (S, S', and S'') 2/6, guaiacyl (G) 2, 5, and 6, and *p*-hydroxybenzoate (PB) 2/6 peaks were observed. As listed in Fig. 4a, the S:G ratio within poplar organosolv lignin were 66:34, closed to those data in other poplar technical lignin [61, 64]. After oxidation, no signals appeared in the aromatic region (Fig. 4b). That meant the degradation and/or modification of the aromatic polymeric units within the heavy fractionation. The absence of aromatic signals in heavy fractionation after oxidation was also confirmed in other catalytic oxidation system [27], whereas it was different with these heavy fractionations from lignin pyrolysis and hydrogenation [62, 63]. After pyrolysis and/or hydrogenation, lignin heavy fractionations also

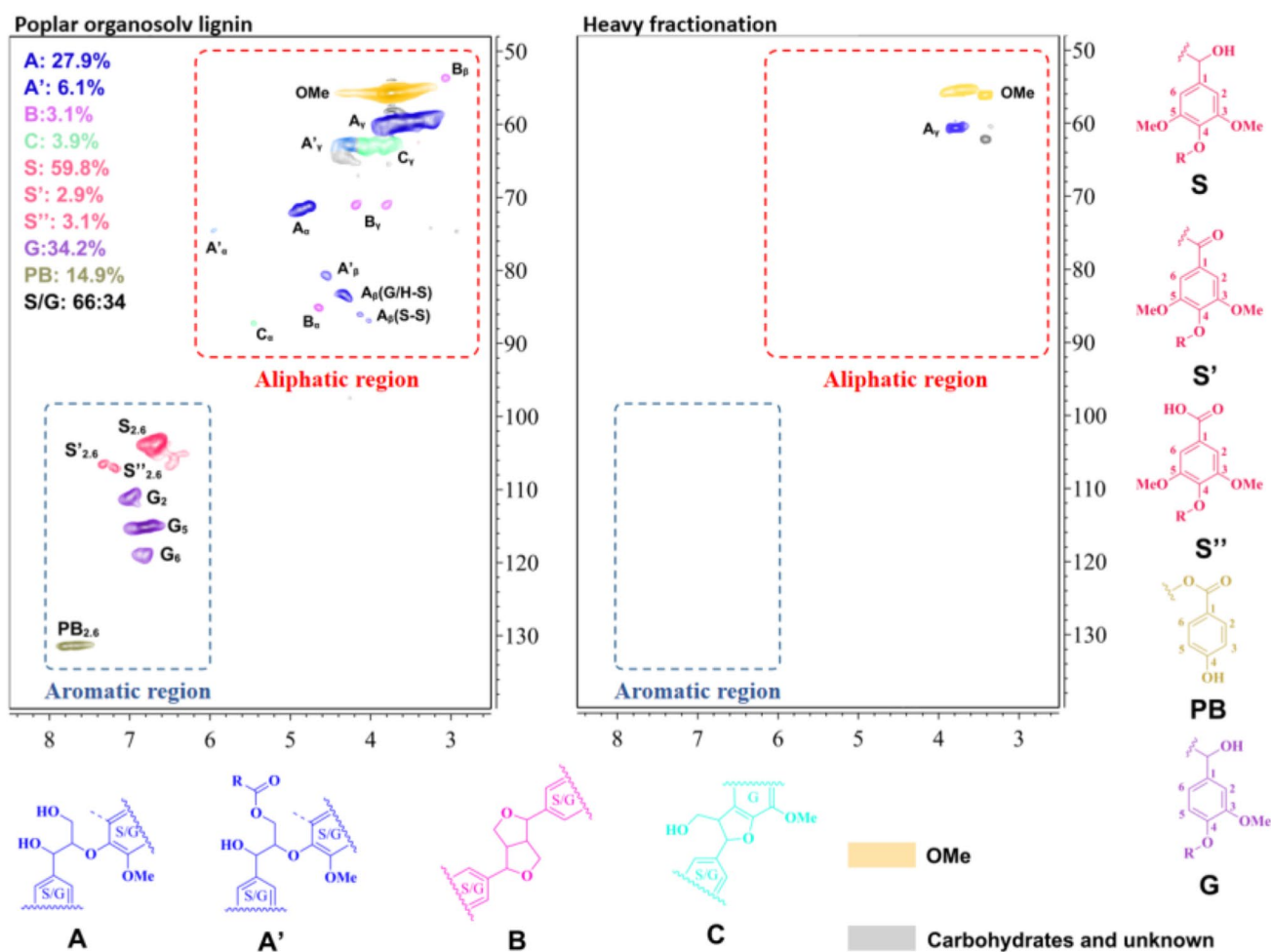


**Fig. 4** HSQC NMR spectra of poplar organosolv lignin and the heavy fractionation after  $\text{VO}(\text{acac})_2$  catalyzed oxidation. Reaction conditions: lignin (0.2 g),  $\text{VO}(\text{acac})_2$  (15 wt.%),  $\text{O}_2$  (1.5 MPa),  $\text{MeCN}/\text{H}_2\text{O}$  co-solvent (15 mL, 1:1, v/v), 140 °C, 48 h, stirring rate 1000 rpm. (A)  $\beta$ -O-4 aryl ether linkages; (A')  $C_\gamma$ -acetylated  $\beta$ -O-4 aryl ether

linkages; (B) resinol substructures formed by  $\beta$ - $\beta$ ,  $\alpha$ -O- $\gamma$ , and  $\gamma$ -O- $\alpha$  linkages; (C) phenylcoumaran substructures formed by  $\beta$ -5 and  $\alpha$ -O-4 linkages; (H) *p*-hydroxyphenyl units; (G) guaiacyl units; (S) syringyl units; (S')  $C_\alpha$ -oxidized syringyl units; (S'') syringic acid end groups

contained some amounts of aromatic and/or their modified signals. Through comparison, we could conclude that lignin molecule was heavily modified during oxidation.

With the cleavage of these ether bonds, especially the  $\beta$ -O-4 linkages, the lignin molecule chain was shortened, and corresponding molecular weight decreased. As shown in Fig. 5 and Table 3, poplar organosolv lignin had only one major peak in the GPC curve at 5170 Da. Whereas the heavy fractionation after oxidation had two shoulder peaks at 930 Da and 490 Da. According to McClelland's method, an approximate degree of polymerization can be calculated with the S:G ratio [63]. The S:G ratio within poplar organosolv lignin was 66:34 (see Fig. 4), so the average molecular weight of a polymeric unit was 218.03 Da for poplar organosolv lignin. Therefore, the major peak of poplar organosolv lignin had a degree of polymerization of 23.7. The degree of polymerization for the heavy fractionation

was 4.3 and 2.2 for the shoulder peaks. In addition, the poplar organosolv lignin had a weight-average molecular weight (Mw) of 5720 Da. After oxidation catalyzed by  $\text{VO}(\text{acac})_2$ , the Mw of heavy fractionation decreased to 1140 Da. The degree of polymerization for poplar organosolv lignin and its heavy fractionation after oxidation was approximately 26.2 and 5.2, respectively. These results meant the poplar organosolv lignin was five-fold oxidative depolymerized, and the heavy fractionation mainly consisted from dimers to pentamers. The polydispersity index of lignin sample decreases from 3.1 to 2.2 after oxidation. The lower polydispersity index of heavy fractionation suggested its better uniformity than poplar organosolv lignin. Our Mw for the heavy fractionation was higher than those in Mottweiler's report [27], whose Mw was only approximately 300 Da. Their Mw data were obtained with the whole oxidized mixture, including monomers, dimers,

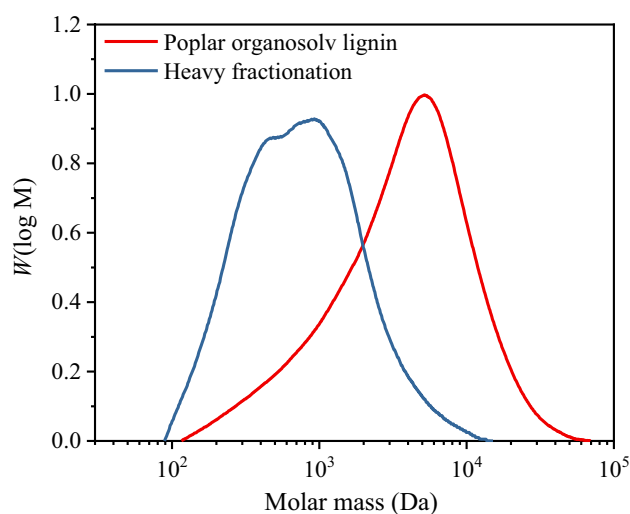


**Fig. 5** GPC mass distribution of poplar organosolv lignin and the heavy fractionation after VO(acac)<sub>2</sub> catalyzed oxidation. Reaction conditions: lignin (0.2 g), VO(acac)<sub>2</sub> (15 wt.%), O<sub>2</sub> (1.5 MPa), MeCN/H<sub>2</sub>O co-solvent (15 mL, 1:1, v/v), 140 °C, 48 h, stirring rate 1000 rpm

**Table 3** Average molecular weights and polydispersity indices of poplar organosolv lignin and the heavy fractionation after VO(acac)<sub>2</sub> catalyzed oxidation

Sample	Mw (Da)	Mn (Da)	Mp (Da)	Polydispersity index
Poplar organosolv lignin	5720	1840	5170	3.1
Heavy fractionation	1140	510	930 & 490	2.2

trimers, oligomers, and so on, whereas our sample was the heavy fractionation precipitated in Et<sub>2</sub>O.

## 4 Conclusions

We investigated the oxidation of lignin and lignin dimers with homogeneous oxovanadium complexes in acetonitrile/water co-solvent under O<sub>2</sub>. In this catalytic oxidation system, β-O-4 lignin dimers were efficiently cleaved, producing aromatic acids and phenols. The catalytic oxidation ability of VO(acac)<sub>2</sub> was higher than that of V(acac)<sub>3</sub>. In addition, oxidation pathways of lignin dimers catalyzed by either VO(acac)<sub>2</sub> or V(acac)<sub>2</sub> should be the same owing to the same monomeric products and observed vanadium changes. Moreover, the produced phenols were proven to be the precursors of condensation. Typical structural features of real lignin, including aromatic and aliphatic functionalities, were heavily degraded in this system, and its molecular chain was five-fold shortened.

**Supplementary Information** The online version contains supplementary material available at <https://doi.org/10.1007/s13399-021-02175-5>.

**Funding** This work was supported by the National Key R&D Program of China (Grant no. 2018YFB1501500), the China Postdoctoral Science Foundation (Grant no. 2020M681454), the Fundamental Research Funds for the Central Universities (Grant no. 2242021R20005), and the Zhishan Postdoctoral Foundation of Southeast University.

## Declarations

**Conflict of interest** The authors declare no competing interests.

## References

- Tuck CO, Perez E, Horvath IT, Sheldon RA, Poliakov M (2012) Valorization of biomass: deriving more value from waste. *Science* 337:695–699
- Li C, Zhao X, Wang A, Huber GW, Zhang T (2015) Catalytic transformation of lignin for the production of chemicals and fuels. *Chem Rev* 115:11559–11624
- Ma R, Guo M, Zhang X (2018) Recent advances in oxidative valorization of lignin. *Catal Today* 302:50–60
- Zakzeski J, Bruijninx PC, Jongerijs AL, Weckhuysen BM (2010) The catalytic valorization of lignin for the production of renewable chemicals. *Chem Rev* 110:3552–3599
- Regalbuto JR (2009) Cellulosic biofuels—got gasoline? *Science* 325:822–824
- Ragauskas AJ, Beckham GT, Biddy MJ, Chandra R, Chen F, Davis MF, Davison BH, Dixon RA, Gilna P, Keller M, Langan P, Naskar AK, Saddler JN, Tschaplinski TJ, Tuskan GA, Wyman CE (2014) Lignin valorization: improving lignin processing in the biorefinery. *Science* 344:1246843
- Lei M, Wu S, Liang J, Liu C (2019) Comprehensive understanding the chemical structure evolution and crucial intermediate radical in situ observation in enzymatic hydrolysis/mild acidolysis lignin pyrolysis. *J Anal Appl Pyrol* 138:249–260
- Sun RC (2020) Lignin source and structural characterization. *Chemsuschem* 13:4385–4393
- Sudarsanam P, Duolikun T, Babu PS, Rokhum L, Johan MR (2020) Recent developments in selective catalytic conversion of lignin into aromatics and their derivatives. *Biomass Convers Bior* 10:873–883
- Y. Fan, C. Liu, X. Kong, Y. Han, M. Lei, R. Xiao, A new perspective on polyethylene-promoted lignin pyrolysis with mass transfer and radical explanation, *Green Energy. Environ.* <https://doi.org/10.1016/j.gee.2021.02.004>.
- Lin F, Liu C, Wang X, Hu C, Wu S, Xiao R (2019) Catalytic oxidation of biorefinery corncob lignin via zirconium(IV) chloride and sodium hydroxide in acetonitrile/water: a functionality study. *Sci Total Environ* 675:203–212
- X. Dou, X. Jiang, W. Li, C. Zhu, Q. Liu, Q. Lu, X. Zheng, H.M. Chang, H. Jameel, Highly efficient conversion of Kraft lignin into liquid fuels with a Co-Zn-beta zeolite catalyst, *Appl. Catal. B: Environ.* 268 (2020) 118429.
- Kong X, Liu C, Han Y, Lei M, Fan Y, Li M, Xiao R (2021) Cu/CuMgAlO<sub>x</sub>-catalyzed guaiacol hydrodeoxygenation in supercritical methanol: a modeling mechanistic insight for lignin-derivatives upgrading. *Energ. Fuel* 35:1511–1522
- Asmadi M, Kawamoto H, Saka S (2011) Gas- and solid/liquid-phase reactions during pyrolysis of softwood and hardwood lignins. *J Anal Appl Pyrol* 92:417–425

15. Zhou S, Xue Y, Sharma A, Bai X (2016) Lignin valorization through thermochemical conversion: comparison of hardwood, softwood and herbaceous lignin. *ACS Sustain Chem Eng* 4:6608–6617
16. Zhang H, Wang Y, Shao S, Xiao R (2016) Catalytic conversion of lignin pyrolysis model compound-guaiacol and its kinetic model including coke formation. *Sci Rep* 6:37513
17. He J, Zhao C, Lercher JA (2012) Ni-catalyzed cleavage of aryl ethers in the aqueous phase. *J Am Chem Soc* 134:20768–20775
18. Zhang J, Asakura H, van Rijn J, Yang J, Duchesne P, Zhang B, Chen X, Zhang P, Saeys M, Yan N (2014) Highly efficient, NiAu-catalyzed hydrogenolysis of lignin into phenolic chemicals. *Green Chem* 16:2432–2437
19. Wang X, Rinaldi R (2012) Solvent effects on the hydrogenolysis of diphenyl ether with Raney nickel and their implications for the conversion of lignin. *Chemsuschem* 5:1455–1466
20. Ma R, Xu Y, Zhang X (2015) Catalytic oxidation of biorefinery lignin to value-added chemicals to support sustainable biofuel production. *Chemsuschem* 8:24–51
21. Liu C, Wu S, Zhang H, Xiao R (2019) Catalytic oxidation of lignin to valuable biomass-based platform chemicals: a review. *Fuel Process Technol* 191:181–201
22. Biannic B, Bozell JJ, Elder T (2014) Steric effects in the design of Co-Schiff base complexes for the catalytic oxidation of lignin models to para-benzoquinones. *Green Chem* 16:3635–3642
23. Mate VR, Jha A, Joshi UD, Patil KR, Shirai M, Rode CV (2014) Effect of preparation parameters on characterization and activity of  $\text{Co}_3\text{O}_4$  catalyst in liquid phase oxidation of lignin model substrates. *Appl Catal A: Gen* 487:130–138
24. Zhu C, Ding W, Shen T, Tang C, Sun C, Xu S, Chen Y, Wu J, Ying H (2015) Metallo-deuteroporphyrin as a biomimetic catalyst for the catalytic oxidation of lignin to aromatics. *Chemsuschem* 8:1768–1778
25. Wang M, Li LH, Lu JM, Li HJ, Zhang XC, Liu HF, Luo NC, Wang F (2017) Acid promoted C-C bond oxidative cleavage of  $\beta$ -O-4 and  $\beta$ -1 lignin models to esters over a copper catalyst. *Green Chem* 19:702–706
26. Zhou ZZ, Liu M, Li CJ (2017) Selective copper-N-heterocyclic carbene (copper-NHC)-catalyzed aerobic cleavage of  $\beta$ -1 lignin models to aldehydes. *ACS Catal* 7:3344–3348
27. Mottweiler J, Puche M, Rauber C, Schmidt T, Concepcion P, Corma A, Bolm C (2015) Copper- and vanadium-catalyzed oxidative cleavage of lignin using dioxygen. *Chemsuschem* 8:2106–2113
28. Wang M, Lu J, Zhang X, Li L, Li H, Luo N, Wang F (2016) Two-step, catalytic C-C bond oxidative cleavage process converts lignin models and extracts to aromatic acids. *ACS Catal* 6:6086–6090
29. Qu C, Ito K, Katsuyama I, Mitani T, Kashimura K, Watanabe T (2020) Directly microwave-accelerated cleavage of C-C and C-O bonds of lignin by copper oxide and  $\text{H}_2\text{O}_2$ . *Chemsuschem* 13:4510–4518
30. Son S, Toste FD (2010) Non-oxidative vanadium-catalyzed C-O bond cleavage: application to degradation of lignin model compounds. *Angew Chem Int Ed Engl* 49:3791–3794
31. Hanson SK, Wu R, Silks LA (2012) C-C or C-O bond cleavage in a phenolic lignin model compound: selectivity depends on vanadium catalyst. *Angew Chem Int Ed Engl* 51:3410–3413
32. Ma Y, Du Z, Liu J, Xia F, Xu J (2015) Selective oxidative C-C bond cleavage of a lignin model compound in the presence of acetic acid with a vanadium catalyst. *Green Chem* 17:4968–4973
33. Mottweiler J, Rinesch T, Besson C, Buendia J, Bolm C (2015) Iron-catalysed oxidative cleavage of lignin and  $\beta$ -O-4 lignin model compounds with peroxides in DMSO. *Green Chem* 17:5001–5008
34. Pan J, Fu J, Lu X (2015) Microwave-assisted oxidative degradation of lignin model compounds with metal salts. *Energ. Fuel* 29:4503–4509
35. Deng W, Zhang H, Wu X, Li R, Zhang Q, Wang Y (2015) Oxidative conversion of lignin and lignin model compounds catalyzed by  $\text{CeO}_2$ -supported Pd nanoparticles. *Green Chem* 17:5009–5018
36. Jiang YY, Yan L, Yu HZ, Zhang Q, Fu Y (2016) Mechanism of vanadium-catalyzed selective C-O and C-C cleavage of lignin model compound. *ACS Catal* 6:4399–4410
37. Zhang G, Scott BL, Wu R, Silks LA, Hanson SK (2012) Aerobic oxidation reactions catalyzed by vanadium complexes of bis(phenolate) ligands. *Inorg Chem* 51:7354–7361
38. Sedai B, Díaz-Urrutia C, Baker RT, Wu R, Silks LAP, Hanson SK (2013) Aerobic oxidation of  $\beta$ -1 lignin model compounds with copper and oxovanadium catalysts. *ACS Catal* 3:3111–3122
39. Parker HJ, Chuck CJ, Woodman T, Jones MD (2016) Degradation of  $\beta$ -O-4 model lignin species by vanadium Schiff-base catalysts: influence of catalyst structure and reaction conditions on activity and selectivity. *Catal Today* 269:40–47
40. Hanson SK, Baker RT, Gordon JC, Scott BL, Silks LA, Thorn DL (2010) Mechanism of alcohol oxidation by dipicolinate vanadium(V): unexpected role of pyridine. *J Am Chem Soc* 132:17804–17816
41. Nichols JM, Bishop LM, Bergman RG, Ellman JA (2010) Catalytic C-O bond cleavage of 2-aryloxy-1-arylethanol and its application to the depolymerization of lignin-related polymers. *J Am Chem Soc* 132:12554–12555
42. Hu J, Wu S, Jiang X, Xiao R (2018) Structure-reactivity relationship in fast pyrolysis of lignin into monomeric phenolic compounds. *Energ. Fuel* 32:1843–1850
43. Liu C, Wang X, Lin F, Zhang H, Xiao R (2018) Structural elucidation of industrial bioethanol residual lignin from corn stalk: a potential source of vinyl phenolics. *Fuel Process Technol* 169:50–57
44. An YX, Li N, Wu H, Lou WY, Zong MH (2015) Changes in the structure and the thermal properties of Kraft lignin during its dissolution in cholinium ionic liquids. *ACS Sustain Chem Eng* 3:2951–2958
45. Lan W, Amiri MT, Hunston CM, Luterbacher JS (2018) Protection group effects during  $\alpha$ ,  $\gamma$ -diol lignin stabilization promote high-selectivity monomer production. *Angew Chem Int Ed Engl* 57:1356–1360
46. Wehrli B, Stumm W (1989) Vanadyl in natural waters: adsorption and hydrolysis promote oxygenation. *Geochim Cosmochim Acta* 53:69–77
47. Rehder D (2008) *Bioinorganic Vanadium Chemistry*. Wiley, Chichester
48. Amin SS, Cryer K, Zhang B, Dutta SK, Eaton SS, Anderson OP, Miller SM, Reul BA, Brichard SM, Crans DC (2000) Chemistry and insulin-mimetic properties of bis(acetylacetonate) oxovanadium(IV) and derivatives I. *Inorg Chem* 39:406–416
49. Nunes CD, Vaz PD, Felix V, Veiros LF, Moniz T, Rangel M, Realista S, Mourato AC, Calhorda MJ (2015) Vanadyl cationic complexes as catalysts in olefin oxidation. *Dalton T* 44:5125–5138
50. Westrup KC, Gregorio T, Stinghen D, Reis DM, Hitchcock PB, Ribeiro RR, Barison A, Back DF, de Sa EL, Nunes GG, Soares JF (2011) Non-oxo vanadium(IV) alkoxide chemistry: solid state structures, aggregation equilibria and thermochromic behaviour in solution. *Dalton T* 40:3198–3210
51. Mota A, Hallett JP, Kuznetsov ML, Correia I (2011) Structural characterization and DFT study of  $\text{V}^{\text{IV}}\text{O}(\text{acac})_2$  in imidazolium ionic liquids. *Phys Chem Chem Phys* 13:15094–15102
52. M.R. Maurya, B. Uprety, F. Avecilla, P. Adao, J. Costa Pessoa, Vanadium(V) complexes of a tripodal ligand, their

- characterisation and biological implications, *Dalton T.* 44 (2015) 17736–17755.
53. Maurya MR, Sarkar B, AVECILLA F, Correia I (2016) Vanadium(IV and V) complexes of pyrazolone based ligands: synthesis, structural characterization and catalytic applications. *Dalton T* 45:17343–17364
  54. Maurya MR, Agarwal S, Abid M, Azam A, Bader C, Ebel M, Rehder D (2006) Synthesis, characterisation, reactivity and in vitro antimicrobial activity of hydrazone based oxovanadium(IV), oxovanadium(V) and  $\mu$ -bis(oxo)bis{oxovanadium(V)} complexes. *Dalton T* 7:937–947
  55. Guo H, Zhang B, Qi Z, Li C, Ji J, Dai T, Wang A, Zhang T (2017) Valorization of lignin to simple phenolic compounds over tungsten carbide: impact of lignin structure. *Chemsuschem* 10:523–532
  56. Sturgeon MR, Kim S, Lawrence K, Paton RS, Chmely SC, Nimlos M, Foust TD, Beckham GT (2013) A mechanistic investigation of acid-catalyzed cleavage of aryl-ether linkages: implications for lignin depolymerization in acidic environments. *ACS Sustain Chem Eng* 2:472–485
  57. Britt PF, Kidder MK, Buchanan AC (2007) Oxygen substituent effects in the pyrolysis of phenethyl phenyl ethers, *Energ. Fuel* 21:3102–3108
  58. Younker JM, Beste A, Buchanan AC III (2011) Computational study of bond dissociation enthalpies for substituted  $\beta$ -O-4 lignin model compounds. *ChemPhysChem* 12:3556–3565
  59. G. Lessene, K.S. Feldman, Oxidative aryl-coupling reactions in synthesis, in: D. Astruc (Ed), *Modern arene chemistry*, Wiley-VCH, Weinheim, 2002.
  60. Wen JL, Sun SL, Xue BL, Sun RC (2013) Recent advances in characterization of lignin polymer by solution-state nuclear magnetic resonance (NMR) methodology. *Materials* 6:359–391
  61. Liu C, Hu J, Zhang H, Xiao R (2016) Thermal conversion of lignin to phenols: relevance between chemical structure and pyrolysis behaviors. *Fuel* 182:864–870
  62. Z. Zhang, B. Du, H. Zhu, C. Chen, Y. Sun, X. Wang, J. Zhou, Facile adjusting the concentration of siliceous seed to obtain different HZSM-5 zeolite catalysts for effective catalytic depolymerization reaction of lignin, *Biomass Conv. Bioref.* (2021). <https://doi.org/10.1007/s13399-021-01352-w>
  63. McClelland DJ, Motagamwala AH, Li Y, Rover MR, Wittrig AM, Wu C, Buchanan JS, Brown RC, Ralph J, Dumesic JA, Huber GW (2017) Functionality and molecular weight distribution of red oak lignin before and after pyrolysis and hydrogenation. *Green Chem* 19:1378–1389
  64. Wang X, Guo Y, Zhou J, Sun G (2017) Structural changes of poplar wood lignin after supercritical pretreatment using carbon dioxide and ethanol-water as co-solvents. *RSC Adv* 7:8314–8322
  65. Lancefield CS, Ojo OS, Tran F, Westwood NJ (2015) Isolation of functionalized phenolic monomers through selective oxidation and C-O bond cleavage of the  $\beta$ -O-4 linkages in lignin. *Angew Chem Int Ed Engl* 54:258–262
  66. Z. Zeng, J. Xie, Y. Guo, R. Rao, B. Chen, L. Cheng, Y. Xie, X. Ouyang, Hydrogenolysis of lignin to produce aromatic monomers over Fe-Pd bimetallic catalyst supported on HZSM-5, *Fuel Process. Technol.* 213 (2021) 106713.
  67. Wang B, Shen XJ, Wen JL, Sun RC (2016) A mild  $\text{AlCl}_3$ -catalyzed ethanol pretreatment and its effects on the structural changes of Eucalyptus wood lignin and the saccharification efficiency. *RSC Adv* 6:57986–57995

**Publisher's note** Springer Nature remains neutral with regard to jurisdictional claims in published maps and institutional affiliations.